Phonon spectra of substitutional carbon in $Si_{1-x}Ge_x$ alloys

L. V. Kulik
Department of Electrical and Computer Engineering, University of Delaware, Newark, Delaware 19716
and Institute of Solid State Physics, RAS, 142432 Chernogolovka, Moscow region, Russia

C. Guedj, M. W. Dashiell, and J. Kolodzey
Department of Electrical and Computer Engineering, University of Delaware, Newark, Delaware 19716

A. Hairie
Laboratoire d'Etudes et de Recherches sur les Materiaux (CNRS UA 6004), Institut des Sciences de La Matiere et du Rayonnement–6, Boulevard du Marechal Juin, 14050 Caen Cedex, France

(Received 28 September 1998; revised manuscript received 19 January 1999)

The phonon spectra of substitutional carbon defects in $Si_{1-x}Ge_x$ alloys are studied over a broad range of Ge contents. With changing composition, the threefold-degenerate localized phonon mode of carbon defects in silicon was found to split into a number of phonon modes. The split-off modes appear due to the warping of defect symmetry while different nearest atomic environments of silicon and germanium atoms form around substitutional carbon atoms. The phonon spectra are simulated with a Keating model, taking into account the effects of carbon anharmonicity. The results of calculations are in good agreement with experiments. [S0163-1829(99)03724-8]

INTRODUCTION

Substitutional carbon in Si and SiGe alloys has attracted substantial interest due to the effects of carbon on the structural, optical, and electronic properties of these semiconductor materials.[1–5] Isolated substitutional and interstitial C defects in silicon have been thoroughly studied both experimentally and theoretically (for a review, see Ref. 6). Conversely, an extensive study of the carbon defect in SiGe alloys has commenced only recently, when nonequilibrium growth techniques such as molecular-beam epitaxy (MBE), chemical vapor deposition, and solid phase epitaxy (SPE) demonstrated carbon concentrations many orders of magnitude in excess of its equilibrium solubility.[7–11]

Because of the significant difference in covalent bond radii between Si and C atoms, the C defect in the Si lattice is surrounded by a considerable strain field, with substitutional defect bonds under tensile strain, and interstitial ones under compressive strain. The minimum formation energy of the interstitial C defect [in a split (100) configuration] exceeds the formation energy of the substitutional C defect by 3 eV,[12] which is why C atoms are favored to occupy substitutional sites.

A substitutional C defect in a SiGe alloy is expected to be surrounded by an even stronger strain field than in pure silicon, due to the increase of the C bond lengths with the Ge atoms. Interstitial C defects will be under smaller compressive strain due to the increase of the average lattice constant with Ge. Thus one could expect a decrease of the energy barrier between substitutional and interstitial C defects in $Si_{1-x}Ge_x$ alloys. The direct support for this was found in Ref. 13, where the thermal stability of substitutional carbon in $Si_{1-x-y}Ge_xC_y$ alloys was measured. The activation energy of substitutional C loss was shown to decrease by more than 1 eV in $Si_{0.7-y}Ge_{0.3}C_y$ alloys compared to $Si_{1-y}C_y$ alloy of similar y values.

Recently, the thermal stability of the substitutional C defect in germanium produced by the SPE technique was reported.[14] The highest obtained ratio of substitutional to total carbon concentration was only 0.3:1, while a similar technique applied to silicon resulted in nearly 100% carbon substitutionality.[15] The substitutional C defects in Ge were detected only in a narrow region of recrystallization temperatures which was far below the stability limit of substitutional carbon in silicon. Combined with previous observations that carbon solubility in germanium is 9–10 orders of magnitude less than in silicon,[16] this indicates that the formation energy of the substitutional C defect in germanium considerably exceeds that in silicon, and the energy barrier between substitutional and interstitial sites in Ge becomes relatively small.

Being of T_d symmetry, the isolated substitutional $C(^{12}C)$ defect in silicon is characterized by a localized threefold-degenerate phonon mode at 605 cm^{-1}, which is Raman and infrared active.[6] If the concentration of C defects becomes high, the interaction between the individual defects results in broadening of the localized phonon mode and weaker satellite phonon modes.[15,17] Intensities of the satellite modes reflect the distribution of the relative C arrangements through silicon, among which the arrangement of C atoms as the third neighbors was especially favorable.[17]

Because of enormous difficulties in diluting any amount of carbon available for optical studies in germanium, the phonon spectrum of substitutional C in germanium was not reported until recently.[14] The localized phonon mode of the isolated substitutional $C(^{12}C)$ defect in germanium has been observed at 531 cm^{-1}.

In the present paper we study the phonon spectra of the substitutional C defect in $Si_{1-x}Ge_x$ alloys, both experimentally using infrared-absorption spectroscopy, and theoretically using an anharmonic Keating model. The phonon frequencies of the substitutional C defect are measured vs Ge content. A number of phonon modes associated with the sub-

 ©1999 The American Physical Society

stitutional C defect are detected, and are attributed to localized phonon modes of C defects with different nearest-neighbor configurations of Si and Ge atoms.

EXPERIMENTAL PROCEDURE

The $Si_{1-x}Ge_xC$ alloys were grown by solid-source MBE on float zone Si(100) substrates. A combination Si-graphite source was used to form a molecular beam of pure Si and Si-C molecular species, resulting in a Si:C ratio of approximately 100:0.8 in the as-grown samples.[18] High-purity Ge was evaporated from a standard effusion source. The Si-graphite source temperature and growth time were held constant for all the samples maintaining a constant Si:C ratio and total number of carbon atoms in the layer. The Ge source temperature was varied to produce $Si_{1-x}Ge_xC$ alloys with increasing Ge content $(0 \leqslant x \leqslant 0.9)$. The substrate temperature was about 200 °C.

The low substrate temperature was chosen to minimize the effects of near-surface diffusion of C atoms. Previous studies of the surface kinetics of C atoms during the MBE growth of $Si_{1-y}C_y$ alloys reveal a thermally activated diffusion of C atoms at the dimerized Si(100) surface from substitutional to near-surface interstitial sites, and conglomeration of C atoms in coherent and incoherent SiC precipitates.[18–20] A similar trend was found during the growth of $Si_{1-x}Ge_xC$ alloys, however, the activation energies and pre-exponential factors differed significantly. For increased Ge concentrations, lower growth temperatures were found to be necessary for a significant incorporation of C atoms in substitutional sites.

The as-grown samples were annealed at 450–750 °C for 30 min to crystallize the as-grown layer. Annealing temperatures were minimized to avoid the bulk diffusion of C atoms to sites other than random substitutional sites (such as the third-neighbor C arrangement mentioned above, and incoherent SiC precipitates). The annealing temperature depended on the stoichometry of the samples, as the activation energy for bulk diffusion of C atoms in $Si_{1-x}Ge_xC$ alloys is a decreasing function of Ge concentration.[13] The asymmetric (224) and symmetric (004) x-ray reflections were applied to quantify the Ge content in the alloy and the tetragonal distortion due to the interface strain between the alloy and substrate.[8,21] The alloys were found to be single crystalline and relaxed at $x > 0.2$. The alloy layers were pseudomorphic for $x \leqslant 0.1$. Alloy layer thickness and annealing temperatures for all values of x studied here are shown in Table I.

The infrared-absorption measurements in the spectral region of the substitutional C vibration mode were performed at room temperature using a Nicolet 740 Fourier-transform infrared spectrometer with a Ga on KBr beam splitter operating in the transmission mode. A globar and a triglycerin sulfide detector were used as a light source and detector, respectively. The instrumental resolution was 1 cm^{-1}. The

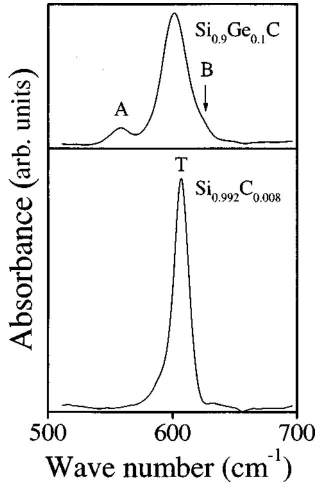

FIG. 1. Differential IR spectra of $Si_{0.992}C_{0.008}$ (bottom) and $S_{0.9}Ge_{0.1}C$ (top) recrystallized alloy samples. The labels *A, B*, and *T* are explained in the text.

small increase of Ge content [Fig. 1 (top)], the main absorption band shifts to lower frequencies and becomes significantly broader. In addition, a satellite band, *A* at 559 cm^{-1} and a shoulder *B* at 625 cm^{-1} become apparent. This trend is consistent with that observed by Hoffman[11] for relaxed $Si_{0.85}Ge_{0.15}$ alloys grown by MBE and implanted with $^{13}C^{+}$ ions for a concentration of $1\times 10^{20}\,cm^{-3}$. For low Ge concentrations ($x<0.20$) they observed both low- and high-frequency absorption lines on either side of the main absorption line of the Si_4 vibration.

The origin of the *A* band was established by investigating the thermal stability of $Si_{0.9}Ge_{0.1}C$ alloys. Figure 2 shows the room-temperature differential IR spectra of the alloy subsequently annealed isothermally at 908 °C for different times. The spectra exhibit absorption bands at 602 and 815 cm^{-1}, and the satellite *A* band at 559 cm^{-1}. The *T* band at 602 cm^{-1} is the local phonon mode of the substitutional C defect,

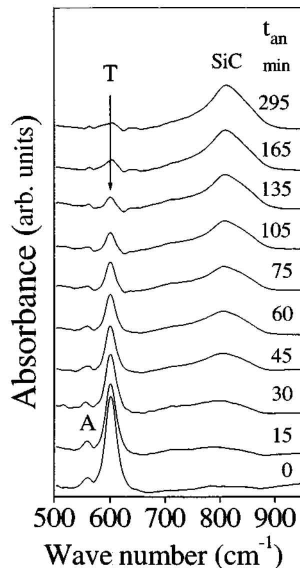

FIG. 2. IR absorbance spectra of the annealing sequence of a $Si_{0.9}Ge_{0.1}C$ alloy sample at 908 °C. Annealing times (t_{an}) are shown in the right side of the figure.

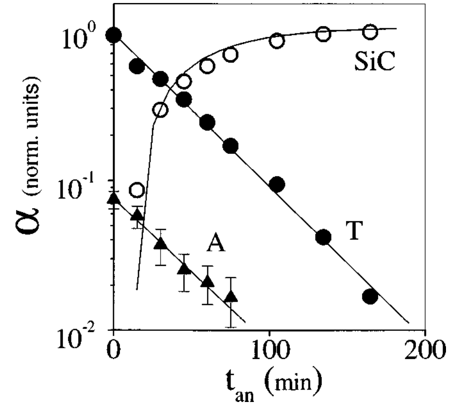

FIG. 3. The integrated IR absorbance (α) vs annealing time of the *T* (solid circles), *A* (triangles), and SiC precipitate (open circles) bands. Solid lines are the best fits of the experimental points.

and the broad asymmetric band at 815 cm^{-1} is associated with the vibration of incoherent SiC precipitates.[15,22] During the annealing sequence, the absorbance of the *T* band decreases and that of SiC precipitates increases, showing that the C atoms transfer from substitutional sites to SiC precipitates.

As C atoms leave substitutional sites, the alloy, being initially strain compensated, gradually becomes compressively strained. We did not observe a frequency shift of the *T* band while the layer strain increased (see Fig. 2). Considering that the C content in $Si_{1-x}Ge_xC$, with $x>0.1$, decreases with increasing x (i.e., the Si:C ratio is constant), we conclude that the partial strain compensation of SiGe layers due to the addition of small fractions of carbon does not observably affect the phonon frequencies of the substitutional C defect.

The integrated absorbance of both *T* and *A* bands versus annealing time is shown in Fig. 3 on a semilogarithmic scale. Also shown is the increase of the absorbance of the broad band centered at 815 cm^{-1}. The decrease of *T* and *A* bands is fit with an exponential decay function:

$$\alpha_{T,A}=\alpha_0 \exp\left\{-\frac{t}{\tau}\right\}, \tag{1}$$

and the increase of the SiC precipitates band with

$$\alpha_{\mathrm{precip}}=\alpha_1\left(1-\exp\left\{-\frac{t}{\tau}\right\}\right). \tag{2}$$

The time constant τ for all three bands is about 45 min within experimental error. As the formation of SiC precipitates is increased by the transfer of C atoms from substitutional sites, we interpreted the equality of the time constants for the growth of the SiC band and the decay of the *A* band as indications of a connection between the *A* band and a C defect. At the same time, having the same temperature stability as the *T* band, *A* is probably associated with a substitution C defect. In favor of this is the fact that interstitial C defects could not possibly account for the *A* band because

TABLE II. Table of Keating parameters used in simulations given in atomic units.

Bond	a_0	α	β
C-C	6.7424	0.143	0.101
Si-Si	10.266 32	0.0637	0.017
Ge-Ge	10.695	0.0555	0.015
Si-C	8.24	0.0555	0.0802
Si-Ge	10.4572	0.053	0.017
C-Ge	8.54	0.0742	0.031

they have a lower temperature stability[2] than substitutional C defects, and rather higher vibration frequencies.[23]

As the A band was not present in the spectrum of the sample without germanium, we attributed this to a phonon mode of a substitutional C defect with one Ge atom involved as the nearest-neighbor (Si_3Ge_1 configuration). This defect holds C_{3V} symmetry, and hence two absorption bands active in IR spectra are to be observed. The possibility of any spectral features relevant to configurations with more than one Ge nearest neighbor should be disregarded at small Ge contents due to the low probability for such configurations to form.

The validity of this assignment was tested by theoretical simulation. We applied a theoretical approach based upon a valence-force-field model derived from Keating, taking into account the effects of carbon anharmonicity. The interactions between atoms have been modeled with an interatomic potential similar to the one of Ref. 24, with the exception of adjusting our force coefficients to yield the correct lattice parameters and phonon modes of silicon, germanium, diamond (in the $Fd3m$ structure), SiGe and 3C-SiC at 300 K. This choice is justified by the very high precision and reliability of these experimental data, which can be obtained by x-ray diffraction, Raman spectroscopy, and absorption spectroscopy at room temperature. Table II displays the equilibrium lattice constants and Keating parameters determined from a least-square fit to the lattice constants and zone-center optical phonons of the corresponding diamond and zinc-blende structures. This set of parameters enables the computation of the LO (Γ) mode from 3C-SiC, which cannot be obtained from the parameters given in Ref. 24 to the best of our knowledge. Our model is therefore ideally suited to a precise computation of the lattice parameters and phonon spectra of tetrahedrally coordinated $Si_{1-x}Ge_xC$ alloys. The molecular-dynamics relaxation is calculated from a 512-atom supercell at time increments of 3 fs until the total potential energy reaches a stable minimum (approximately 2000 fs). We have computed isotropic relaxations, where no external pressure is applied to the computational box, to simulate a fully relaxed layer on silicon. In a further stage, the local phonon density around carbon is computed, using the recursion method detailed in Ref. 25. We have chosen to compute the local phonon spectra around carbon atoms situated near the center of the supercell to avoid surface effects. For each Ge concentration, several Si_aGe_b configurations of the carbon nearest neighbors were tested so that a particular configuration was held fixed, and the remaining atoms in the computation box were distributed randomly. The spectra were averaged over 16 random distributions.

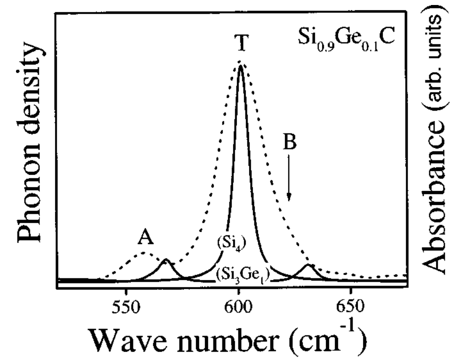

FIG. 4. Simulated localized phonon density around C (solid line), together with the measured IR absorbance spectrum (dots) for $x=0.1$. The relative populations if the two configurations Si_4 and Si_3Ge_t were determined by assuming that the probability to find a Ge or Si atom next to C is equal.

The simulated localized phonon density around C, together with the measured IR spectrum for $x \sim 0.1$ is shown in Fig. 4.[26] The simulation yielded the mode at T for the local vibrational mode (LVM) of C in Si_4. The simulated A and B modes are due to the low-frequency nondegenerate and high-frequency doubly degenerate phonon mode of the Si_3Ge_1 configuration, respectively. The phonon frequency of the substitutional C defect with the four Si nearest neighbors (Si_4) is close to the experimental position of the T-band maximum. The lower-frequency nondegenerate phonon mode of the experimental Si_3Ge_1 defect slightly exceeds (by 8 cm^{-1}) the frequency of the A-band maximum. We did not experimentally observe a separately resolved absorption band corresponding to the simulated high-frequency twofold-degenerate phonon mode of the Si_3Ge_1 defect. It may be that the frequency of this mode partly overlaps the frequency of the Si_4 defect phonon mode, and thus accounts for the observed high frequency shoulder of the T band, B, at 625 cm^{-1} (Fig. 4).

Upon a further increase of the Ge content, the effects of interference fringes on the IR spectra of $Si_{1-x}Ge_xC$ alloys become considerable, and we could no longer use the standard differential technique. As an example, the differential spectra of a $Si_{1-x}Ge_xC$ ($x \sim 0.79$) alloy grown on a Si substrate before (dots) and after long-time annealing (dashed line) are shown in Fig. 5. The differential spectra are not straightforward for interpretation due to interference fringes; however, a relative differential spectrum (solid line), which is a difference between the recrystallized and annealed spectra, is well defined.

Figure 6 shows a set of relative differential spectra of $Si_{1-x}Ge_xC$ alloys at $0 \leqslant x \leqslant 0.54$. The spectra are characterized by two absorption bands T and A, shifting linearly to low frequencies upon increase of the Ge content, with the slopes of -0.53 ± 0.3 and $-0.56 \pm 0.4\ cm^{-1}$ per 1% of germanium, respectively. The shift of the T band is in close agreement with the simulations, which give linear slope of $-0.57\ cm^{-1}$ per 1% of germanium.

Because of the C-C interaction, the full width at half maximum (FWHM) of the T band at $x=0$ is as much as 12 cm^{-1}, which is twice that of the individual substitutional C defect in silicon (6 cm^{-1}). At $x=0.1$, the FWHM of the T band becomes even broader ($\sim$20 cm^{-1}). This broadening is

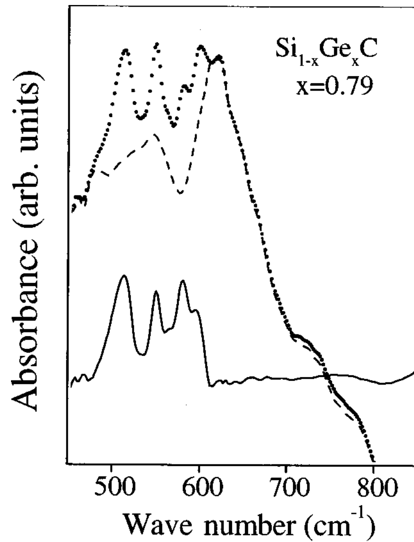

FIG. 5. Differential spectra of a $Si_{1-x}Ge_xC$ alloy for $x \sim 0.79$ before (dots) and after long-time annealing (dashed line). The relative differential spectrum is shown by the solid line.

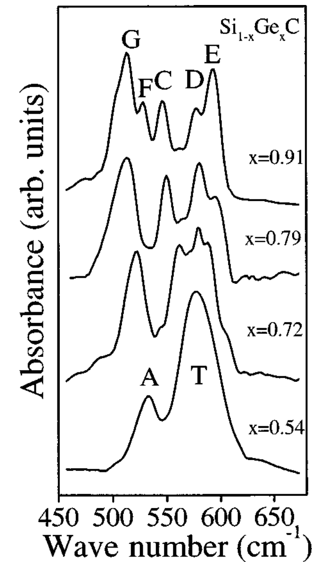

FIG. 7. Relative differential absorbance spectra of $Si_{1-x}Ge_xC$ alloys for $0.54 \leq x \leq 0.91$.

accounted by the effects of different *second*-neighbor, *third*-neighbor, etc. configurations, but not the *first*-neighbor configuration on the phonon frequency of the substitutional C defect in the alloy. It is not therefore surprising that the FWHM of the *A* band is of the same value, as the effect of remote neighbors is similar for substitutional C defects in both Si_4 and Si_3Ge_1 configurations.

The expected behavior of the *T*- and *A*-band FWHM's with increasing Ge content is determined by two opposing tendencies:(1) broadening due to the different second-neighbor, etc. configurations to achieve a maximum around $x \sim 0.5$, and (2) narrowing due to reduction of the C-C interaction (our growth method preserves the SiC ratio, hence effectively increasing the average distance between C atoms in the alloys with increasing Ge content). The FWHM of the *A* band achieves a maximum at $x \sim 0.3$, and then starts decreasing, showing that the second tendency indeed becomes dominating, see the inset of Fig. 6.

The *T*-band FWHM, however, behaves differently than expected. Having been equal to that of *A* band up to $x = 0.23$, the FWHM starts increasing and achieves as much as 36 cm^{-1} at $x \sim 0.54$ (the inset to Fig. 6). The only possible explanation for this huge broadening is that the *T* band no longer represents the phonon mode of substitutional C defect in one particular configuration, but appears to be a composite band. This becomes obvious from Fig. 7, where the relative

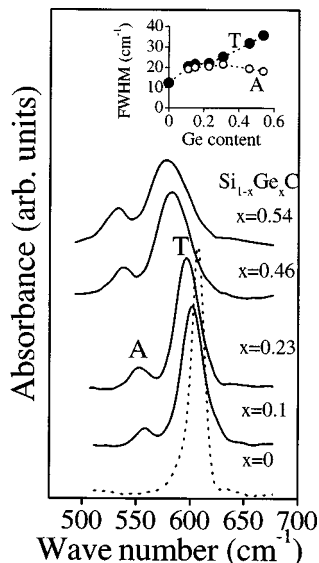

FIG. 6. Relative differential IR absorbance spectra of $Si_{1-x}Ge_xC$ alloys for $0 \leq x \leq 0.54$. In the inset, the full width at half maximum of the *T* and *A* bands are shown.

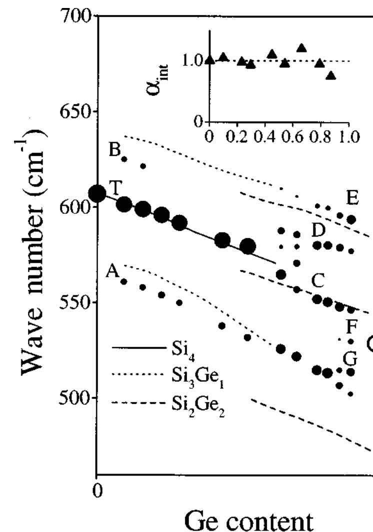

FIG. 8. Frequencies of the observed IR-absorption bands (solid circles) labeled in Fig. 7 vs Ge content. The dot areas reflect the integrated absorbance of each band determined by separately fitting each line to a Gaussian, followed by integration of the Gaussian fit. The lines are simulated frequencies of the localized phonon modes of substitutional C defects in particular nearest-neighbor configurations. The open circle at $x = 1$ is the localized phonon mode frequency of the substitutional C defect in germanium. The inset shows the integrated absorbance through all IR-absorption bands associated with the substitutional C defect.

differential IR spectra of $Si_{1-x}Ge_xC$ alloys at higher Ge contents are shown.

The broad *T* absorption band splits into a number of narrow ones at $x>0.6$. At first, two bands, *C* and *D*, develop in the IR spectra (Fig. 7). Their relative absorbance stays nearly constant with increasing Ge content, which points out that both bands are associated with two phonon modes of the same defect. Having considered that the next statistically favorable substitutional C defect after the Si_3Ge_1 configuration has to be the Si_2Ge_2 one, we concluded that the *C* and *D* bands were associated with the two phonon modes of the substitutional C defect in the Si_2Ge_2 configuration. It holds a C_{2V} symmetry; hence three IR-active phonon modes are to be observed. The third expected mode has not yet been detected. It is quite possible that an absorption band corresponding to the third phonon mode is not resolved from the *A* band. In fact, the *A* band expands nearly twice in the narrow region of Ge contents, $0.54<x<0.7$, which may be interpreted as the contribution of two absorption bands associated with the substitutional C defect in the Si_3Ge_1 and Si_2Ge_2 configurations, overlapping in the same spectral region. Simulations made for the C defect in the Si_2Ge_2 configuration demonstrate that the two calculated phonon modes of the Si_2Ge_2 defect are best matched to the *C* and *D* bands, but the third phonon mode frequency situates noticeably below the frequency of *A* band.

At the highest Ge contents, an absorption band *F* develops in the IR spectra, with a frequency, if approximated to $x=1.0$, that tends to the frequency of the localized C phonon mode in pure germanium (Figs. 7 and 8). It was therefore attributed to the localized phonon mode of the substitutional C defect in the Ge_4 configuration. The rest of the observed absorption bands (*E* and *G*) dominating the IR spectra at the highest Ge contents, $x>0.8$, were tentatively assigned to the two IR-active phonon modes of the Si_1Ge_3 defect (Figs. 7 and 8).

Along with the frequencies of the observed absorption bands, we studied the total integrated absorption coefficient of all the absorption bands associated with substitutional C defects as a function of Ge content, shown in the inset to Fig. 8. Within experimental error, it is almost preserved through all Ge contents. This remarkable fact directly confirms the conclusion of Ref. 14, that the effective charge of the substitutional C atom in germanium has a similar value as in silicon. Moreover, this conclusion is now extended to $Si_{1-x}Ge_x$ alloys correspondingly. It could only be so if the effective charge of substitutional C in $Si_{1-x}Ge_x$ alloys does not significantly depend on the C-atom neighbors.

CONCLUSION

The phonon spectra of substitutional C defects in $Si_{1-x}Ge_x$ alloys are studied both experimentally and theoretically. The effect of symmetry warping due to different *first*-neighbor, *second*-neighbor, etc. configurations of Si and Ge atoms around substitutional carbon on the phonon spectra of the defect is discussed. It is found that the effective charge of the substitutional C atom in $Si_{1-x}Ge_x$ is not affected significantly by the C-atom neighbors. The theoretical model developed in Ref. 19 for the simulation of phonon spectra of $Si_{1-x}Ge_xC$ alloys is tested for broad regions of Ge contents. Close agreement between experimental and theoretical results is obtained.

ACKNOWLEDGMENTS

This work was supported by the Army Research Office under Grant No. DAAH04-95-1-0625 and Grant No. AASERT DAAG55-97-1-0249, by the Defense Advanced Research Projects Agency under Contract No. F49620-96-C-0006, and by the Office of Naval Research under Grant No. N00014-93-1-0393.

[1] G. Davies and R. C. Newman, in *Handbook on Semiconductors*, edited by T. S. Moss (Elsevier Science, Amsterdam, 1994), Vol. 3b, p. 1557, and references therein.
[2] G. D. Watkins and K. L. Brower, Phys. Rev. Lett. **36**, 1329 (1976).
[3] L. W. Song, X. D. Zhan, B. W. Benson, and G. D. Watkins, Phys. Rev. Lett. **60**, 460 (1988).
[4] O. F. Sankey, A. A. Demkov, W. T. Petuskey, and P. F. McMillan, Modell. Simul. Mater. Sci. Eng. **1**, 741 (1993).
[5] P. C. Kelires, Phys. Rev. Lett. **75**, 1114 (1995).
[6] R. C. Newman, Adv. Phys. **18**, 544 (1969).
[7] K. Eberl, S. S. Iyer, S. Zollner, J. C. Tsang, and F. K. LeGoues, Appl. Phys. Lett. **60**, 3035 (1992).
[8] B. Dietrich, H. J. Osten, H. Rücker, M. Methfessel, and P. Zaumseil, Phys. Rev. B **49**, 17 185 (1994).
[9] A. St. Amour, C. W. Liu, J. C. Sturm, Y. Lacroix, and M. L. W. Thewolt, Appl. Phys. Lett. **67**, 3915 (1995).
[10] J. W. Strane, H. J. Stein, S. R. Lee, B. L. Doyle, S. T. Picraux, and J. M. Mayer, Appl. Phys. Lett. **63**, 2786 (1993).
[11] L. Hoffman, J. C. Bach, J. L. Hansen, A. N. Larsen, B. B. Nielson, P. Leary, R. Jones, and S. Oberg, in *Defects in Semiconductors ICDS-19*, edited by G. Davies and M. H. Nazare, [Mater. Sci. Forum **258–263**, 97 (1997)].
[12] J. Tersoff, Phys. Rev. Lett. **74**, 5080 (1995).
[13] L. V. Kulik, D. A. Hits, M. W. Dashiell, and J. Kolodzey, Appl. Phys. Lett. **72**, 1972 (1998).
[14] L. Hoffman, J. C. Bach, B. Bech Nielsen, P. Leary, R. Jones, and S. Öberg, Phys. Rev. B **55**, 11 167 (1997).
[15] J. W. Strain, H. J. Stein, S. R. Lee, S. T. Picraux, J. K. Watanabe, and J. W. Mayer, J. Appl. Phys. **76**, 3656 (1994).
[16] R. I. Scace and G. A. Slack, J. Chem. Phys. **30**, 1551 (1959).
[17] H. Rücker, M. Methfessel, B. Dietrich, K. Pressel, and H. J. Osten, Phys. Rev. B **53**, 1302 (1996).
[18] M. W. Dashiell, L. V. Kulik, D. A. Hits, J. Kolodzey, and G. Watson, Appl. Phys. Lett. **72**, 833 (1998).
[19] C. Guedj, M. W. Dashiell, L. V. Kulik, J. Kolodzey, and A. Hairie, J. Appl. Phys. **84**, 4631 (1998).
[20] H. J. Osten, E. Bugiel, and P. Zaumseil, Appl. Phys. Lett. **64**, 3440 (1994).
[21] M. Fatemi and R. E. Stahlbush, Appl. Phys. Lett. **58**, 825 (1991).
[22] J. Mi, P. Warren, P. Letourneau, M. Judelewicz, M. Gailhanou,

M. Dutoit, C. Dubois, and J. C. Dupuy, Appl. Phys. Lett. **67**, 259 (1995).
[23] A. R. Bean and R. C. Newman, Solid State Commun. **8**, 175 (1970).
[24] H. Rücker and M. Methfessel, Phys. Rev. B **52**, 11 059 (1995).
[25] A. Hairie, F. Hairie, G. Nouet, E. Paumier, and A. P. Sutton, in *Polycrystalline Semiconductors III–Physics and Technology*, edited by H. P. Strunk, J. H. Werner, B. Fortin, and O. Bonnaud (Trans Tech, Zurich, 1993). Vols. 37 and 38, p. 91.
[26] The calculated phonon densities give only a rough measure of the intensities of the absorption lines associated with local vibrational modes.